INFRARED LINE EMISSION FROM PLANETARY NEBULAE

Thomas N. Delmer and Robert J. Gould

Department of Physics

University of California , San Diego

and

William Ramsay, UCSD

INFRARED LINE EMISSION FROM PLANETARY NEBULAE

I. GENERAL THEORY

THOMAS N. DELMER and ROBERT J. GOULD

Department of Physics

University of California, San Diego

and

WILLIAM RAMSAY

Department of Physics

University of California, Santa Barbara

ABSTRACT

The general physical processes are considered which determine the intensities of infrared emission lines resulting from magnetic dipole transitions between fine structure levels in certain abundant ions. Methods for calculating the ionization equilibrium from data on optical line intensities are developed. Radiative recombination is treated in some detail and general results are given for averaged recombination Gaunt factors. Helium radiative recombination line intensities are computed. By means of the quantum defect method, some additional important collision strengths are calculated. Estimates of the infrared line spectra for a number of planetaries are presented in a following paper.

I. INTRODUCTION

Recently it has become clear that a large amount of the radiation emitted from interstellar HII regions is in the form of far infrared line radiation. The infrared emission lines result from transitions between the different J-levels of the ground state terms of ions with $2p^n$ and $3p^n$ configurations; these fine structure splittings are usually about $\Delta E \sim 0.01 - 0.1$ eV. The important transitions are all of the magnetic dipole type with $\Delta J = \pm 1$; quadrupole transitions for which $\Delta J = \pm 1, \pm 2$ are much weaker. For example, the ratio of allowed quadrupole to allowed magnetic dipole intensities at a wavelength $\lambda \sim 15\mu$ is $I_q/I_m \sim (a_o/\alpha\lambda)^2 \sim 10^{-7}$, where a_o is the Bohr radius and α is the fine structure constant. The principal mechanism for the excitation of upper fine structure levels is inelastic electron collisions; the levels are easily excited by this process, since for typical interstellar HII regions and nebulae the incident electron energies are $E_e \sim kT_e \sim 1$ eV $\gg \Delta E$.

Some preliminary investigations (Gould 1966) have shown that one can expect to observe these infrared lines from planetary nebulae and a program to carry out such observations has now been started by F. C. Gillett and W. A. Stein of the University of California, San Diego and F. J. Low of the University of Arizona. It is because of these planned observations that the present work was undertaken. Our aim is to calculate, on the basis of data obtained from optical observations, the expected intensities of the observable infrared line spectrum of the brightest planetaries. The results of these calculations are given in the following paper (II). The usefulness of observations of these infrared lines does not appear to have been generally realized. In addition to providing information on the general structure of planetaries, valuable

information on element abundances could be obtained from measurements of infrared line intensities. This is especially so since elements are found in several stages of ionization in planetaries, and in some cases it is difficult if not impossible to measure the abundances of certain ions by observing optical spectra. An example is the ion Ne^+ which has no low-lying optical levels (and so no electron collision induced forbidden optical lines) but which has a low-lying fine structure level and an associated observable infrared line. Moreover, we should like to emphasize that generally the atomic parameters (cross section or collision strength and radiative transition probability) can be calculated more accurately for transitions between fine structure levels than for transitions between optical levels. This is because there exists a general method, the so-called Quantum Defect Method (QDM, see Sect. III), which can be applied very well to collisional excitation of fine structure levels, even though the energies ($\sim$ 1 eV) of the incident electrons are small compared to the energies ($\sim$ 10 eV) of the atomic electrons. Also, the radiative transition probability can be computed very easily and accurately for magnetic dipole transitions between fine structure levels (Sect. III). Finally, it should be mentioned that the dependence of the infrared line production rate on assumed electron temperature is much weaker than for optical line production. Thus, the excitation and emission processes are well understood and accurate element abundances could be derived from accurate measurements of infrared line intensities.

In most cases collisional (rather than radiative) de-excitation of upper fine structure levels can be neglected, so that the rate of production of infrared photons from transitions in an ion i is essentially proportional to the volume integral of the product $n_i n_e$, where n_e is the electron density. Since the product $n_p n_e$ of the proton and electron densitities

integrated over the volume of the ionized region of the planetary nebula can be found from, say, the absolute Hβ flux, the problem of calculating the flux J_i in an infrared line from the ion i is essentially one of determining the mean abundance $\langle n_i/n_p \rangle$ of the ion relative to ionized hydrogen. The general problem of the ionization equilibrium (or steady state) in planetaries is considered in the following section (II); in this section we also consider some related problems of more general interest such as the problem of determining the temperatures of central stars in planetaries. We also give some general results applicable to the problem of the helium abundance. The last section (III) of this paper is devoted to the problem of level population of fine structure states. In this section the basic infrared excitation processes are treated in some detail and results are given of calculations of important associated atomic parameters.

While we shall go into detail on certain problems, we have not tried to make improved determinations of general element abundances, although this could be done by making full use of all the recent photoelectric observational data. It is our hope that this can be done much better when the infrared observations are completed.

We concentrate our attention on the calculation of the expected intensities of 11 infrared lines (see following paper) which, it appears, should be observable from below the atmosphere because of the 7-14μ, 17-24μ and other "windows" at shorter wavelengths. The 9 ions involved are O IV, Ne II, Ne V, Mg IV, S III, S IV, A III, A V, and A VI.

II. IONIZATION EQUILIBRIUM

In this section we consider some of the basic atomic processes which determine the ionization structure of planetary nebulae. We have found the two excellent reviews by Seaton (1960) and Osterbrock (1964) very useful in our work. Most of the older work on planetary nebulae may be found in the collection of papers[1] assembled by Menzel (1962). Recent work on this problem has been done by Hummer and Seaton (1963, 1964), Hummer (1963), Harmon and Seaton (1966) and Seaton (1966). Ionization equilibrium results from a balance of photoionization by uv radiation from the central star of the planetary and radiative capture. Thus, it is determined by the local electron density n_e and the effective temperature T_o and dilution factor W of the stellar radiation field. Our general aim here is to outline methods of determining (essentially semi-emperically) the mean ionization of certain elements on the basis of observations of the ionization of other elements (for example oxygen and helium for which there are usually extensive data).

[1] It is unfortunate that this compilation did not include any of the older papers by Seaton and Spitzer and their collaborators which we shall be referring to.

a) Photoionization

Consider the rate constants (in sec^{-1}) γ_A and γ_B for photoionization of the species A and B (ionization energies: I_A and I_B) at a given point in a planetary nebula, assumed optically thin to the ionizing radiation. If the temperature of the radiation field is T_o and the radiation is a diluted blackbody field we have, if I_A/kT_o , $I_B/kT_o \gg 1$, (see Burbidge, Gould and Pottasch 1963, hereinafter referred to as "BGP"; Gould 1966)

$$\frac{\gamma_A}{\gamma_B} \approx \frac{\sigma_A I_A^2 \exp(-I_A/kT_o)}{\sigma_B I_B^2 \exp(-I_B/kT_o)} \quad , \tag{1}$$

where σ_A and σ_B are the threshold photoionization cross sections. The principal assumption here is that a single temperature characterizes the spectral (blackbody) shape of the radiation field. The model atmosphere calculations of Böhm and Deinzer (1965) have shown that the deviations from a blackbody distribution can be large for photon energies greater than the HeII-Ly edge (54.4 eV). However as long as one is not applying equation (1) when I_A and I_B are on opposite sides of this edge, the error involved should not be very great. Of course, results of employing the expression (1) should be most accurate if $I_A \approx I_B$, since then the error due to the uncertainty in T_o is minimal. In part (d) of this section we shall outline methods for the determination of T_o from optical line intensity data.

An essential quantity required for these relative ionization calculations is the threshold photoionization cross section which in some cases, namely for ionized species, cannot be determined experimentally. Unfortunately, photoionization cross sections are very hard to calculate, due to the oscillatory nature of the integrand in the associated "bound-free" matrix element. Nevertheless, a number of calculations of photoionization cross sections have been made for complex ions. Results of these calculations are summarized by Seaton (1958); an additional compilation including some experimental results has been given by Dichtburn and Öpik (1962). We have computed some additional threshold photoionization cross sections by the quantum defect method as developed by Burgess and Seaton (1960). For these calculations we have employed the improved calculations of Peach (1966) and get σ_z = 0.1, 20, 1, 0.2, 10, 2, 4, 0.8 x 10^{-18} cm for z = Mg^+, S^+, S^{+2}, S^{+3}, A^+, A^{+2}, A^{+3}, A^{+4}

respectively. The essential idea in the method is to relate the phase in the wave function of the ejected electron to the extrapolated value $\mu'(0)$ (principal quantum number $n \to \infty$) of the quantum defects in the pertinent $n^{2S+1}L$ series of the bound levels of the species before ionization. Of course, for some ions, especially the highly ionized species, very little data exists on the high atomic energy levels, and the extrapolated quantum defects cannot be determined accurately. Moreover, as Burgess and Seaton have emphasized, in some cases the calculated value of the cross section depends strongly on the adopted value of $\mu'(0)$. This is so in all of the above cases when σ_z is small; therefore, these values are inaccurate and could easily be off by a factor of three, in our opinion. In all cases we have quoted only one significant figure for σ_z. This reflects our general skepticism of all calculations of photoionization cross sections for complex ions.

b) Radiative recombination

We consider first the case of recombination of purely hydrogenic ions $a^{+(z)}$ of charge z: $a^{+(z)} + e \to a^{+(z-1)} + \gamma$ (γ : photon). The number of these recombinations per cm^3 per second into levels of principal quantum number n (summation over orbital and azimuthal quantum numbers ℓ and m is implied) is $\alpha_{n,z} n_e n_z$, where n_e and n_z are the electron and $a^{+(z)}$ number densities respectively and $\alpha_{n,z}$ is the recombination coefficient. For an electron gas of temperature T_e, $\alpha_{n,z}$ is given by (cf. BGP, Spitzer 1948)

$$\alpha_{n,z} = 2A(2kT_e/\pi m)^{\frac{1}{2}} y\, \varphi_n(y)\, \langle \bar{g}_{z,n} \rangle_{T_e} \quad ; \qquad (2)$$

here $A = 2^5\, 3^{-3/2}\, \alpha^3\, \pi\, a_o^2 = 2.105 \times 10^{-22}\ cm^2$ ($\alpha = 1/137$; a_o = Bohr radius), $y = z^2 I_H/kT_e \equiv z^2\beta_e$, $\varphi_n(y)$ is the transcendental function[2]

[2] We use the notation of BGP; note that therein the exponent of (-x) in eq. (A4b) should be r instead of r-1.

$$\varphi_n(y) = (y/n^3)\, e^{y/n^2} \int_{y/n^2}^{\infty} u^{-1}\, e^{-u}\, du \quad , \tag{3}$$

and $\langle \bar{g}_{n,z} \rangle_{T_e}$ is an effective Gaunt factor, averaged over ℓ and over the velocity distribution of the incident electrons.

Temperature averaged Gaunt factors have been computed by Glasco and Zirin (1964). However, we have found their tables to be inadequate for our general purposes. We require recombination coefficients for z up to 4 and since temperature averaged hydrogenic Gaunt factors are functions of T_e/z^2 (Gaunt factors are equal for equal values of T_e/z^2), a little reflection reveals

$$\langle \bar{g}_{z,n} \rangle_{T_e} = \langle \bar{g}_{1,n} \rangle_{T_e/z^2} \quad . \tag{4}$$

Therefore, the temperature averaged Gaunt factor for an ion z may be found by taking the value for hydrogen (z=1) at a temperature T_e/z^2 (not $z^2 T_e$ as Glasco and Zirin say). It would be very useful if the Glasco-Zirin tables were extended to lower temperatures.

The recombination rate is essentially proportional to the mean value of $1/v_e$, the reciprocal of the incident electron velocity. Since the Gaunt factor is a slowly varying function of electron energy we have approximated the temperature average by the value of the Gaunt factor at the effective energy E_{eff} corresponding to this v_e:

$$\langle \bar{g}_{z,n} \rangle_{T_e} \approx \bar{g}_{z,n}(E_{eff}) \; ; \quad E_{eff} = \pi kT/4 \; . \tag{5}$$

We have taken the Gaunt factors from Karzas and Latter (1961). Comparison with some of the Glasco-Zirin tables indicates that this procedure should be accurate to better than 1%.

In a number of instances we require the total recombination rate to all levels, say, $n > k$. For this recombination rate constant we write

$$\alpha_z^{(k)} = 2A\,(2kT_e/\pi m)^{\frac{1}{2}}\, y\, \varphi^{(k)}(y)\ \langle \bar{g}_z^{(k)} \rangle_{T_e,n} \tag{6}$$

here

$$\varphi^{(k)}(y) \equiv \sum_{n=k}^{\infty} \varphi_n(y)\ , \tag{7}$$

and the last factor in equation (6) is an appropriately averaged (over n) Gaunt factor. Clearly the weighting factors in this further averaging are the φ_n which have the asymptotic expansion (BGP)

$$\varphi_n(y) \rightarrow (1 - n^2/y + \cdots)/n\ . \tag{8}$$

Moreover, for large n, $\varphi_n(y)$ is small ($\propto n^{-1}$) also, most of the contribution to the total recombination rate (6) comes from $n \lesssim \sqrt{y} = \sqrt{\beta_e}\, z$ (by eq. [8]). Thus we take

$$\langle \bar{g}_z^{(k)} \rangle_{T_e,n} \approx \sum_{n=k}^{\sqrt{y}} n^{-1}\, \langle \bar{g}_{z,n} \rangle_{T_e} \Bigg/ \sum_{n=k}^{\sqrt{y}} n^{-1} \tag{9}$$

We give values of this quantity for $T_e = 0.5$, 1.0, and 2.0×10^4 °K in Table 1; at these temperatures $\sqrt{y} = 6z$, $4z$, and $3z$ respectively. For the values enclosed in parentheses in this table, the sum (9) consisted of only one term.

The function $\varphi^{(k)}(y)$ may be found from the tabulation of Spitzer (1948, wherein it is denoted by $\varphi_k(y)$) or in some cases from the analytic formula derived by BGP. By the general procedures outlined here the recombination rates can be calculated to an accuracy of better than 1% which is at least as good as other methods devised such as that of Seaton (1959). In addition, our method would seem to have more general usefulness. Perhaps the calculations could be made even more accurately if Spitzer's (1948) tables were computed to one more significant figure and if the Glasco-Zirin tables were extended.

For the radiative recombination of complex ions $a^{+(z)} + e \rightarrow a^{+(z-1)} + \gamma$ in which the principal quantum number of the outer electrons of $a^{+(z-1)}$ in the ground state is k we take a hydrogenic approximation for the radiative capture rate. That is, we take an expression of the form (6) with $\varphi \langle \bar{g} \rangle$ replaced by (see Elwert 1954, Tucker and Gould 1966).

$$\varphi \langle \bar{g} \rangle = \varphi^{(k+1)}(y) \langle \bar{g}_z{}^{(k+1)} \rangle_{T_{e,n}} + (\bar{\zeta}_k/2k^2) \varphi_k(y) \langle \bar{g}_{z,k} \rangle_{T_e} \quad ; \qquad (10)$$

here $\bar{\zeta}_k$ is the number of <u>holes</u> in the k-shell of $a^{+(z)}$. The averaged $\bar{g}$'s may be taken from Table 1 and from Karzas and Latter (1961). Calculations of recombination rates by this procedure are probably accurate to about 20%.

c) Hydrogen and Helium Recombination Spectrum

The recombination spectrum of atomic hydrogen has been computed by Burgess (1958) and more recently and accurately by Pengelly (1964). In these treatments only radiative processes are considered; effects of collisional transitions have been investigated by Pengelly and Seaton (1964) and are found to be of minor importance except for very high levels. By solving the capture-cascade equations Pengelly has calculated the rate of emission of

energy per cm^3 in the form of the Balmer lines. A convenient analytic expression for this emission as a function of temperature is, for a Balmer Hn line,

$$I(H{:}n \rightarrow 2) = n_e n_p \varepsilon_n = n_e n_p A_n T_e^{-\frac{1}{2}} \ell n \beta_e , \qquad (11)$$

where $\beta_e = I_H/kT_e$, n_e and n_p are the electron and proton (ionized hydrogen) densities, and the A_n are constants. BGP have shown that this one-parameter (A_n) fit should give the approximate temperature dependence of this line emission rate. Actually, on comparison with Pengelly's calculations of the Hβ emission we find that, to the accuracy of his calculations, the form (11) gives exactly his computed ratio of emission at 2×10^4 °K to emission at 1×10^4 °K. Thus, certainly for Hβ emission, we expect equation (11) to describe very accurately the temperature dependence of emission. By comparison with Pengelly's calculations for "case B" (Lyman lines optically thick, the likely state in planetaries) at 10^4 °K we derive the values $A_\beta = 0.449 \times 10^{-23}$ erg-cm^3-$(^oK)^{\frac{1}{2}}$-sec^{-1}, and $A_\alpha = 1.290 \times 10^{-23}$, $A_\gamma = 0.209 \times 10^{-23}$, $A_\delta = 0.115 \times 10^{-23}$, $A_\varepsilon = 0.071 \times 10^{-23}$, $A_\zeta = 0.047 \times 10^{-23}$ in the same units.

For the calculation of line intensities resulting from capture to and cascade in HeI we take a hydrogenic approximation for the excited level structure of HeI in principal quantum number. Using the definition of the hydrogenic $b_{n\ell}$ (cf. Pengelly 1964) which give measures of the n^ℓ level population, we can write, in the hydrogenic approximation,[3]

[3] This procedure is slightly different from that of Seaton (1960) who calculates the photon production rate or "effective recombination coefficient" in this manner and then computes the line intensity using the exact wavelengths of the helium lines.

$$\frac{I(\text{HeI: } n^{2S+1}L \rightarrow n'^{2S+1}L')}{I(\text{H: } n \rightarrow n')} =$$

$$\frac{2S+1}{4} \quad \frac{b_{nL}(2L+1)\, A(n,L \rightarrow n', L')}{\sum_{L=0}^{n-1} \sum_{L'=0}^{n'-1} b_{nL}\,(2L+1)\, A(n,L \rightarrow n', L')} \qquad (12)$$

In equation (12) the b's are the hydrogenic values computed by Pengelly (1964); the A's, the radiative transition probabilities per unit time, can be found from the hydrogenic dipole matrix elements tabulated by Green, Rush, and Chandler (1957). The HeI recombination line intensities can be written (see eq. [11])

$$I(\text{HeI: } i \rightarrow j) = n_e n_{He^+} \varepsilon_{ij} \quad , \qquad (13)$$

where we find, for example, $\varepsilon_{ij} = 5.18 \times 10^{-26}$ erg-cm^3-sec^{-1} at $T_e = 10^4$ ^oK for the line λ4471: $4^3D \rightarrow 2^3P$. We give in Table 2 the relative intensities of other strong helium triplet lines calculated in the same manner along with a calculation of the λ10829 line intensity; the calculations are for $T_e = 10^4$ ^oK and the dependence on temperature should be very weak. The λ10829: $2^3P \rightarrow 2^3S$ line intensity is computed by calculating the total rate of population of the 2^3P level, since this level depopulates only by transition to 2^3S. We compute this by including the effects of direct radiative capture to 2^3P and cascade transitions from n^3S and n^3D with $n > 3$; this cascade population of 2^3P is computed in the hydrogenic approximation as in equation (12). The results given in Table 2 are compared with those of Pottasch (1962) with which the agreement is fairly good except for the λ7065 line. In this case our result seems to agree generally better with the recent observations of O'Dell (1963a). While there seems to be wide variations (often amounting

to a factor ~ 2) among planetaries in the observational helium line ratios (which is hard to understand theoretically, unless it is due to collisional processes) the calculated intensity ratios in Table 2 are in overall agreement with the observations with the exception of λ10829. Perhaps for this infrared line the atmospheric extinction corrections are very critical; O'Dell's (1963a) observations of NGC 6543, 6826, 7027, 7662, and IC 418 give intensity ratios of 2.3, 6.3, 41, 47, and 42 respectively for the intensity ratio $\lambda 10829/\lambda 4471$.

Our main interest in the observations of the helium recombination spectrum is in the information it provides on the helium ionization structure (and thus the general ionization structure) of the planetary and in the application to the determination of the central star temperature of the planetary. For these problems it is necessary to determine the relative amount of doubly-ionized helium. This can be done from an analysis of the HeII recombination spectra and in particular from a measurement of the intensity of the strong line λ4686 HeII:4 $\rightarrow$ 3. The energy emitted per cm^3 in this line is $n_e n_{He^{+2}} \varepsilon_{43}$; with $\varepsilon_{43} = 1.58 \times 10^{-24}$ erg-cm^3-sec^{-1} at $T_e = 10^4$ °K as calculated by Pengelly (1964). This allows the determination of the abundance of ionized helium relative to ionized hydrogen in planetaries. Using the results of calculations at 10^4 °K we find[4]

[4] There seems to be a rather large discrepancy in the coefficient of the relation (14) determining $n_{He^{+2}}/n_{H^+}$ and the value given by Harmon and Seaton (1966). Our number is based on Pengelly's calculations which were also cited by Harmon and Seaton. The fact that their calculations are for $T_e = 1.5 \times 10^4$ °K cannot explain the discrepancy. Needless to say, we have checked our result.

$$\frac{\langle n_e n_{He^+} \rangle}{\langle n_e n_{H^+} \rangle} = 2.39 \frac{I(HeI:\lambda 4471)}{I(H\beta:\lambda 4861)} \quad ; \tag{14}$$

$$\frac{\langle n_e n_{He^{+2}} \rangle}{\langle n_e n_{H^+} \rangle} = 0.0785 \frac{I(HeII:\lambda 4686)}{I(H\beta:\lambda 4861)} \quad .$$

Note that it is not the average relative abundances He^+/H^+ and He^{+2}/H^+ which are determined in this manner but the ratio of the average abundances weighted by the local electron density. Thus in a planetary in which there are large density variations the total ionized helium to hydrogen ratio cannot be determined accurately.

d) Central Star Temperature

The effective temperature of the radiation field at a given point in a planetary nebula is an essential parameter which determines the ionization conditions therein. This is so essentially because of the exponential dependence [see eq. (1)] of the photoionization rate on temperature. Determinations of the temperatures T_o of central stars of a number of planetary nebulae have been made recently by O'Dell (1963b) and by Harmon and Seaton (1966). The basic methods involved in these determinations are due originally to Zanstra (1931, 1960) and the essential idea is the following: (1) the apparent magnitude or intensity of the stellar emission continuum at some particular wavelength or wavelength band is compared with the intensity of some particular line of, say, the hydrogen recombination spectrum, or (2) the intensity of a hydrogen recombination line is compared with the intensity of a line of, say, the recombination spectrum of neutral helium. The point is that the total production rate of the recombination line is directly related to the total recombination rate which in turn is equal to the total number of

photons emitted per second from the central star with energy greater than the ionization energy of the recombined species. Thus, the ratio of the observed quantities in both method (1) and (2) are independent of the distance to the planetary and of the radius of the central star. For the determination of the central star temperature we have employed the second method (2), since for some planetaries, for example NGC 7027, the central star has not been identified. On the assumption that all the ionizing photons emitted by the central star are absorbed in the nebula we can write

$$\frac{\langle n_e n_{H^+} \alpha_{H^+} \rangle}{\langle n_e n_{He^+} \alpha_{He^+} \rangle} = \frac{N_i(H)}{N_i(He)} \quad , \tag{15}$$

where the average is over the volume of the ionized matter, the α's are the recombination coefficients and the N_i's are the number of photons emitted per second by the central star which ionize the species. We make the assumption that a fraction φ of the H-ionizing photons from the star are absorbed in the gas and an identical fraction (φ) of the He-ionizing and He^+-ionizing photons are absorbed. Since the nebula often does not completely surround the central star this fraction is not always unity (see Harmon and Seaton 1966). Further, we assume, in all cases, that photons of energy greater than 4Ry are absorbed only by He^+, and photons of energy between 1.807Ry and 4Ry and between 1Ry and 1.807Ry are absorbed by He and H respectively. The ionization problem is complicated by the effect of the ionization of atomic hydrogen by photons from the $2^1S \rightarrow 1^1S$ two-photon emission continuum in He. As a result, about 60% (see Hummer and Seaton 1963) of the photons which ionize He-atoms result in recombination and cascade photons which ionize H-atoms. Similarly, some of the 2s - 1s continuum of He^+ ionizes

He. However, we neglect this last effect; the relative number of these photons compared to the He-ionizing stellar photons is small since $N_i(He^+)/N_i(He)$ is approximately proportional to $\exp[-(4-1.807)Ry/kT_o]$ $\ll 1$ (usually). Thus we assume this number is always small, so that

$$\frac{N_i(H)}{N_i(He)} = \frac{F_i(x_H) - 0.4\, F_i(x_{He})}{F_i(x_{He})} \tag{16}$$

$$\frac{N_i(He)}{N_i(He^+)} = \frac{F_i(x_{He})}{F_i(x_{He^+})} \quad ,$$

where

$$F_i(x_z) = \int_{x_z}^{\infty} \frac{x^2 dx}{e^x - 1} \quad , \quad x_z = I_z/kT_o \; . \tag{17}$$

The function F_i can be found from the "Debye function" tabulated by Abromowitz and Stegun (1965). These relations can then be substituted into equations of the form (15) where the left hand side can be determined from the observed line ratios as in equation (14). In the calculation of the recombination coefficients we count only captures to excited states, assuming the photons from direct capture to the ground state just ionize other atoms of the same species. By equation (6) we find, at $T_e = 10^4\ ^oK$, $\alpha_{H^+} = \alpha_{He^+} = \alpha_1^{(2)} = 2.52 \times 10^{-13}\ cm^3\ sec^{-1}$, $\alpha_{He^{+2}} = \alpha_2^{(2)} = 1.50 \times 10^{-12}\ cm^3\ sec^{-1}$.

We shall apply these relations to the determination of T_o's in the following paper. We might mention here that the exact value of φ, the fraction of the ionizing photons that are absorbed in the nebula, does not come in to the analysis if it is the same for the ionization of H, He^+, and He^+. For this

reason the method may be superior to that of O'Dell and Harmon and Seaton (op.cit.) in which the method (1) is employed. We shall compare our results for T_o with theirs.

The recent work by Böhm and Deinzer (1965) who computed the spectral distribution of the stellar radiation field from model central stars of planetary nebulae must be mentioned. Based on model atmosphere calculations, they found appreciable deviation from a blackbody form, especially beyond $\hbar\omega = 4$Ry at which they found (for a star of $T_o = 10^5\ ^oK$) a reduction of about an order of magnitude in the spectral emission; this is due to absorption by He^+ in the stellar atmosphere. We have not corrected for this effect. As a result, temperatures determined from HeII recombination line intensities may be on the high side.

III. LEVEL POPULATION AND LINE EMISSION

a) Level Population

The energy emitted per cm^3 per second from a transition from state i to state j in atom a is

$$I(a:i \rightarrow j) = n_{ai} A_{ij}(E_i - E_j) \quad , \tag{18}$$

where E_i and E_j are the corresponding energies of the fine structure levels, A_{ij} is the radiative transition probability per unit time for $i \rightarrow j$ and n_{ai} is the number of atoms per cm^3 in the state i. The transitions considered here are of the magnetic dipole type with $\Delta J = \pm 1$, and the associated A_{ij} can be computed easily from the general formula derived by Shortley (1940) for LS coupling conditions. The $n_i(a)$ is then the quantity to be calculated; it can be found by writing down the condition for a steady state (Seaton 1960): the number of (collisional and radiative) transitions

to level $\underline{i}$ from all other levels is equal to the number of transitions from this level. Let w_i denote the fractional population of level $\underline{i}$ and P_{ik} the transition probability per unit time for $\underline{i} \rightarrow \underline{k}$. Here

$$P_{ik} = n_e q_{ik} + A_{ik} \quad , \tag{19}$$

where n_e is the electron density, $q_{ik} = \langle \sigma_{ik} v_e \rangle$ is the electron collisional rate constant, and the radiative transition probability A_{ik} is zero if $E_k > E_i$. Then the steady state condition is

$$w_i \sum_k P_{ik} = \sum_k w_k P_{ki} \quad , \quad \sum_i w_i = 1 \quad . \tag{20}$$

By detailed balance q_{ik} and q_{ki} are related by

$$q_{ik}/q_{ki} = (\omega_k/\omega_i) \exp\left[(E_i - E_k)/kT_e\right] \quad , \tag{21}$$

where the ω's are the degeneracies $(2J + 1)$ of the levels. In our application we consider only transitions within the same optical term which is always the ground state term. The total number of fine structure levels within this term is either two $(J = \frac{1}{2}, \frac{3}{2})$ (denoted here by 1 and 2) or three $(J = 0, 1, 2)$. In the case of two levels with $E_1 < E_2$ equation (20) is simply

$$\frac{w_2}{w_1} = \frac{w_2}{1-w_2} = \frac{n_e q_{12}}{n_e q_{21} + A_{21}} \tag{22}$$

which approaches $n_e q_{12}/A_{21}$ and $(\omega_2/\omega_1) \exp[(E_2 - E_1)/kT_e]$ in the low and high density limit respectively. For the case of three levels the specific expressions are much more complicated. However, in the high density limit the relative population number approaches the equilibrium value

$w_i \rightarrow \omega_i \exp(-E_i/kT_e) \Big/ \sum_i \omega_i \exp(-E_i/kT_e)$. In our case where radiative de-excitation is predominantly by magnetic dipole emission with $\Delta J = \pm 1$, radiative transitions are to the level directly below since always $E_J < E_{J+1}$ (or the reverse). Then if the levels are ordered according to their energy, we can write in the low density limit where collisional deexcitation is negligible and where the ground state is predominantly populated

$$I(a:i \rightarrow j) \rightarrow n_e n_{ao} (E_i - E_j) \sum_{k=i}^{m} q_{ok} , \quad \text{(low density)} \tag{23}$$

here o denotes the ground state and m the highest fine structure level. That is, every collisional excitation to a level higher than i produces, in the cascade, an $i \rightarrow j$ photon. On the other hand, at high densities

$$I(a:i \rightarrow j) \rightarrow n_{aT} (E_i - E_j) A_{ij} \frac{\omega_i \exp(-E_i/kT_e)}{\sum_i \omega_i \exp(-E_i/kT_e)} , \quad \text{(high density)} \tag{24}$$

here $n_{aT} = \sum_i n_{ai}$ is the total density of the atom a . It should be noted that in the low density limit the emission per unit volume goes as the square of the density while at high densities it is proportional to the density. The collisional rate constant q_{ij} can be written in a convenient form if the collision strength Ω_{ij} is defined, where, in terms of the electron collision cross section σ_{ij} ,

$$\sigma_{ij} = \pi \Omega_{ij} / \omega_i (p/\hbar)^2 , \tag{25}$$

where p is the momentum of the incident electron. Then, on the assumption

that Ω_{ij} is independent of the energy of the incident electron, one finds, on integrating over a Maxwellian electron velocity distribution, for deexcitation ($E_i > E_j$),

$$q_{ij} = C\,\Omega_{ij}/\omega_i T_e^{1/2} \tag{26}$$

where $C = (2\pi/k)^{1/2}\,\hbar^2 m^{-3/2} = 8.63 \times 10^{-6}$ cm^3 sec^{-1}($^\circ$K)$^{1/2}$; excitation rates q_{ji} can then be found from equation (21). Calculation of Ω_{ij} is most easily performed with the help of the quantum defect method discussed in part (b) of this section.

As illustrative examples of the electron density dependence of the population of fine structure levels we give in Figure 1a and 1b the results of calculations of the population of fine structure levels in the ground state terms of O IV and S III . There are two levels ($J = \frac{1}{2}$ and $\frac{3}{2}$) in the system O IV and three levels ($J = 0$, 1, and 2) in S III; the ground states of these species are $O^{+3} : 2p\ ^2P_{1/2}$ and $S^{+2} : 3p^2\ ^3P_0$. These are examples of systems from which infrared photons are emitted (see the following paper) and illustrate the characteristic densities where the changeover occurs from the low to high density condition. The calculations were performed for a gas with an electron temperature $T_e = 10^4\ ^\circ$K. We then plot the relative populations w_i as a function of electron density. In Figure 1a for O IV we have plotted the relative population $w_{3/2}$ of the upper ($J = \frac{3}{2}$) state; the population of the ground state is just $w_{1/2} = 1 - w_{3/2}$. The dashed lines in the figure denote the populations in the low and high density limit or approximation; at high densities the relative populations are the equilibrium values which are independent of density; in fact, for the electron temperatures we consider, $E_i/kT_e \ll 1$, and the high density limits reflect essentially the relative

degeneracies. For the case of the three levels in S III (Fig. 1b) the dependence on density is more complicated; in fact, the relative population of the middle level $J = 1$ shows a maximum at $n_e \approx 8 \times 10^3$ cm^{-3}. This effect of a pile-up in this level occurs in other ions besides S III and results essentially from the relatively long lifetime for the $J = 1 \rightarrow 0$ radiative transition relative to that for $J = 2 \rightarrow 1$. We show as the dashed lines in Fig. 1b also the low and high density limits to the relative populations w_0, w_1, and w_2. We should like to emphasize that, as Figures 1a and 1b show, the characteristic densities at which the dependence on density is strong (or where collisional deexcitation is important) is, for some infrared lines, $\sim 10^4$ cm^{-3}, that is, typical planetary nebula densities. This means that by infrared observational methods of this type electron densities could be determined.

b) Collision Strengths - the QDM

The line emission per cm^3 can be calculated from equations (18), (19) and (20) once the collision strengths Ω_{ij} for the inelastic processes are known for the elements involved. Some of these collision strengths have been taken from calculation or estimates by Seaton (1958), Osterbrock (1965), and Blaha (1964). We have calculated those which were not available, using the popular quantum defect method (cf. Seaton, loc. cit.). The basis of this method is the fact that the partial-wave phase shift for low-energy elastic electron-ion scattering is equal, in the limit of zero electron energy, to $\pi\mu'(E)$, where $\mu'(E)$ is the quantum defect for the system of electron plus ion extrapolated through the ionization limit to positive energies. In practice, the extrapolation from available level data may be difficult or impossible, and observed $\mu'(-|E|)$ must be used.

It should be emphasized that the method as developed applies in the elastic limit in that the fine structure levels of different J are approximated as being degenerate. This is also assumed in setting equal to unity the coefficient of $\exp(2i\delta)$ in the partial wave cross section, implying equality of the total probability current for the incident and scattered electron. Because of this inherent approximation the method should not be valid for very slow collisions, say for a thermal gas where $kT_e \lesssim \Delta E$, where ΔE is the level separation. For our application $kT_e \sim 1$ eV $\gg \Delta E$; however, one would be led to question the application of the result of the method to the calculation of collisional cooling by this process in HI regions where $kT_e \sim 10^{-2}$ eV (cf. Seaton 1955a).

In the QDM applied to scattering the S-matrix for scattering from states $J \rightarrow J'$ is transformed by means of 9-j coefficients to a representation suitable for using the quantum-defect-derived elastic phase shifts. The procedure is described by Seaton (1958) and Osterbrock (1965). Table 3 gives the results of our calculation.

The collision strength for the $\frac{1}{2} \rightarrow \frac{3}{2}$ process in Mg IV was calculated using the formulas given in Osterbrock (1965); note that in his Ω^{ss}, π_i should be read for σ_i. The quantum defects were derived from the lower, Russell-Saunders-like, levels of Mg III (Moore, 1958). s, p, and d partial cross sections are calculated from the observed spectra and the contributions for other ℓ were estimated by the distorted wave method, using an atomic radius kindly supplied by P. J. Kelly (private communication).

The collision strength for the A VI $\frac{3}{2} \rightarrow \frac{1}{2}$ transition was not calculated because there were too few quantum defects available. This ion is, however, a member of the isoelectronic sequence treated by Blaha (1964); the

Vainshtein relation discussed by him can be used to estimate the A VI collision strength. Of course, the value obtained is only very approximate: As Blaha points out, the Vainshtein relation does not seem to hold very well for the Si II isoelectronic sequence.

Collision strengths for the ions with three ground fine structure levels were calculated as described above with the 9-j coefficients for $J = 0 \rightarrow 1$, $1 \rightarrow 2$, $0 \rightarrow 2$ transitions (Smith and Stevenson 1957). s-, p- and d-wave quantum defects were available (Moore 1958) for S III and A III; other partial waves were estimated as described above using Hartree-Fock $\langle r^2 \rangle$ values (Czyzak 1962, Kelly private communication). The case of A V was somewhat less satisfactory: d-waves were not available, and the contribution from the d-waves was so important in the other two cases that the calculated A V results seemed suspect. This was so, especially, because the distorted-wave-tail (Seaton 1955b) contribution for d-waves is large for $0 \rightarrow 2$ and $1 \rightarrow 2$ transitions and zero for $0 \rightarrow 1$. In the presence of this uncertainty, the calculated values for $1 \rightarrow 2$ and $0 \rightarrow 2$ were accepted as estimates and the other transition, $0 \rightarrow 1$, was scaled up from the S III results. From what we have just said, the difficulties of applying the quantum defect method must be evident. For many ions, one is indeed fortunate to find <u>one</u> set of d-wave defects; the method, however, really requires an <u>extrapolated</u> value: in cases where such an extrapolation <u>is</u> possible, the initial and the limiting quantum defects are often significantly different from each other. This comment should not be taken as ingratitude in the face of the development of a method which gives at least some information where there was none before. Nevertheless, we think it is misleading to guess at d-wave quantum defects and then (as has happened) quote the resulting collision strength to four significant figures. This <u>caveat</u> applies to our Table (3):

the A V and A VI results are indicated as estimates, as discussed above. In addition, however, the other calculated values are good only as long as the f-wave contributions are small (probably a good assumption - see Osterbrock 1965) and as long as the observed quantum defects for low n are close to the extrapolated defect. When phrased just as stated, the last is a rather poor assumption; however, there may be a saving grace that only the differences between defects occur in the collision strength: hopefully these differences are somewhat less sensitive to extrapolation than the values themselves. At any rate, we recommend caution in the use of the quantum defect method.

TABLE 1. AVERAGED RECOMBINATION GAUNT FACTORS

$\langle \bar{g}_z^{(k)} \rangle_{T_{e,n}}$ $(T_e = 0.5 \times 10^4\ ^\circ K)$

z \ k	1	2	3	4
1	0.882	0.937	0.960	0.974
2	0.893	0.938	0.956	0.966
3	0.899	0.940	0.956	0.965
4	0.905	0.944	0.958	0.967

$\langle \bar{g}_z^{(k)} \rangle_{T_{e,n}}$ $(T_e = 1.0 \times 10^4\ ^\circ K)$

z \ k	1	2	3	4
1	0.877	0.939	0.967	(0.983)
2	0.885	0.934	0.954	0.967
3	0.892	0.936	0.954	0.964
4	0.897	0.939	0.954	0.964

$\langle \bar{g}_z^{(k)} \rangle_{T_{e,n}}$ $(T_e = 2.0 \times 10^4\ ^\circ K)$

z \ k	1	2	3	4
1	0.878	0.947	(0.978)	(1.008)
2	0.883	0.937	0.960	0.975
3	0.888	0.936	0.956	0.968
4	0.893	0.938	0.956	0.966

TABLE 2. CALCULATED* HeI RECOMBINATION LINE INTENSITY RATIOS

Line	Intensity Ratio	
	Present Work	Pottasch (1962)
$\lambda 4026 : 5^3D \rightarrow 2^3P$	0.46	0.53
$\lambda 4471 : 4^3D \rightarrow 2^3P$	1.00	1.00
$\lambda 5876 : 3^3D \rightarrow 2^3P$	2.75	2.80
$\lambda 7065 : 3^3S \rightarrow 2^3P$	1.77	0.46
$\lambda 10829 : 2^3P \rightarrow 2^3S$	5.50	4.01

* for 10^4 °K

TABLE 3. CALCULATED COLLISION STRENGTHS

(See text for discussion of accuracy)

ion	J,J′	$\Omega_{JJ'}$
Mg IV	$\frac{1}{2}$, $\frac{3}{2}$	0.31
A VI	$\frac{1}{2}$, $\frac{3}{2}$	3 (estimated)
S III	0, 1	2.1
	1, 2	4.2
	0, 2	0.7
A III	0, 1	1.8
	1, 2	4.3
	0, 2	0.96
A V	0, 1	3 (estimated)
	1, 2	4
	0, 2	2

REFERENCES

Abramowitz, M. and Stegun, I. A. 1965, Handbook of Mathematical Functions (New York: Dover Publications Inc.).

Blaha, M. 1964, Bull. Astron. Inst. Czechoslovakia, 15, 33.

Böhm, K. H. and Deinzer, W. 1965, Z. Ap., 61, 1.

Burbidge, G. R., Gould, R. J. and Pottasch, S. R. 1963, Ap. J. 138, 945.

Burgess, A. 1958, M. N., 118, 477.

Burgess, A. and Seaton, M. J. 1960, M. N., 120, 121.

Czyzak, S. J. 1962, Ap. J. Suppl. No. 65.

Ditchburn, R. W. and Öpik, U. 1962, Atomic and Molecular Processes, Bates, D. R., Ed., p. 79 (New York: Academic Press).

Elwert, G. 1954, Z. Naturforsch., 9a, 637.

Glasco, H. P. and Zirin, H. 1964, Ap. J. Suppl. 9, 193.

Gould, R. J. 1966, Ap. J., 143, 603.

Green, L. C., Rush, P. P., and Chandler, C. D. 1957, Apr. J. Suppl. 3, 37.

Harmon, R. J. and Seaton, M. J. 1966, M. N., 132, 15.

Hummer, D. G. 1963, M. N., 125, 461.

Hummer, D. G. and Seaton, M. J. 1963, M. N., 125, 437.

_____ 1964, ibid., 127, 217.

Karzas, W. J. and Latter, R. 1961, Ap. J. Suppl., 6, 167.

Menzel, D. H. 1962, Selected Papers on Physical Processes in Ionized Plasmas (New York: Dover Publications).

Moore, C. E. 1949, Atomic Energy Levels, Vol. 1, NBS Circ. 467.

O'Dell, C. R. 1963a, Ap. J., 138, 1018.

_____ 1963b, ibid., p. 67.

Osterbrock, D. E. 1964, Ann. Rev. Astron. and Astrophys., 2, 95.

_____ 1965, Ap. J., 142, 1423.

Peach, G. 1966, M. N. (in press).

Pengelly, R. M. 1964, M. N., 127, 145.

Pengelly, R. M. and Seaton, M. J. 1964, M. N., 127, 165.

Pottasch, S. R. 1962, Ap. J., 135, 385.

Seaton, M. J. 1955a, Ann. d'ap, 18, 188.

_____ 1955b, Proc. Roy. Soc. (London), A231, 37.

_____ 1958, Rev. Mod. Phys. 30, 979.

_____ 1959, M. N., 119, 81.

_____ 1960, Rept. Prog. Phys., 23, 313.

_____ 1966, M. N., 132, 113.

Shortley, G. H. 1940, Phys. Rev., 57, 225.

Smith, K. and Stevenson, J. W. 1957, Argonne Natl. Lab. Rep. ANL - 5776.
Spitzer, L., Jr. 1948, Ap. J., 107, 6.
Tucker, W. H. and Gould, R. J. 1966, Ap. J., 144, 244.

Zanstra, H. 1931, Publ. Dom. Ap. Obs. (Canada), 4, 209.

_____ 1960, B. A. N., 15, 237.

FIGURE CAPTIONS

Fig. 1a. Relative population $w_{3/2}$ of the $J = \frac{3}{2}$ level in O IV as a function of electron density n_e for $T_e = 10^4\ ^\circ K$. The low and high density limit approximations to $w_{3/2}$ are shown as dashed lines.

Fig. 1b. Relative populations of the $J = 0$, 1, and 2 levels in S III as a function of electron density n_e for $T_e = 10^4\ ^\circ K$. The low and high density approximations are shown as dashed lines.

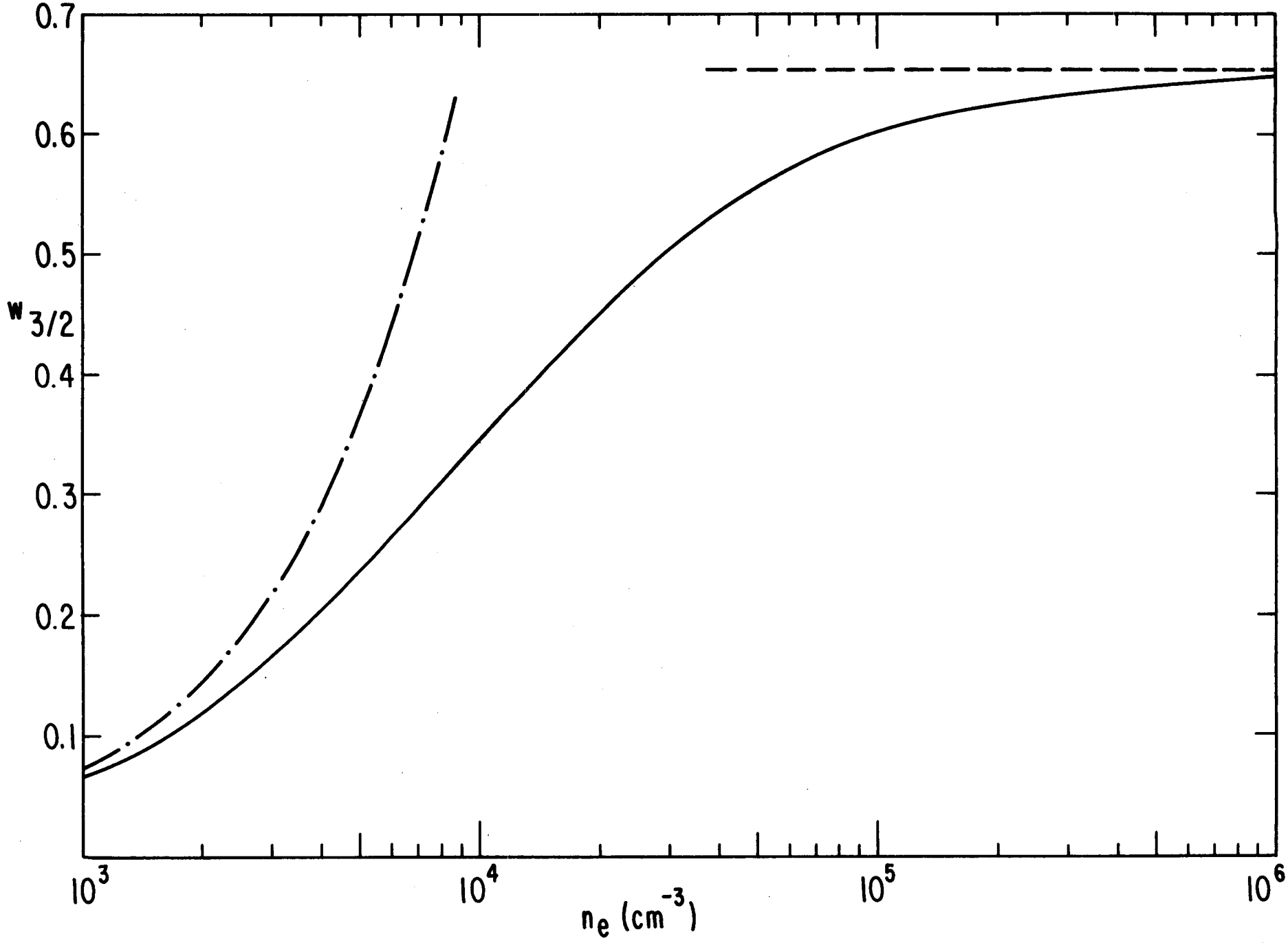

Fig. 1a

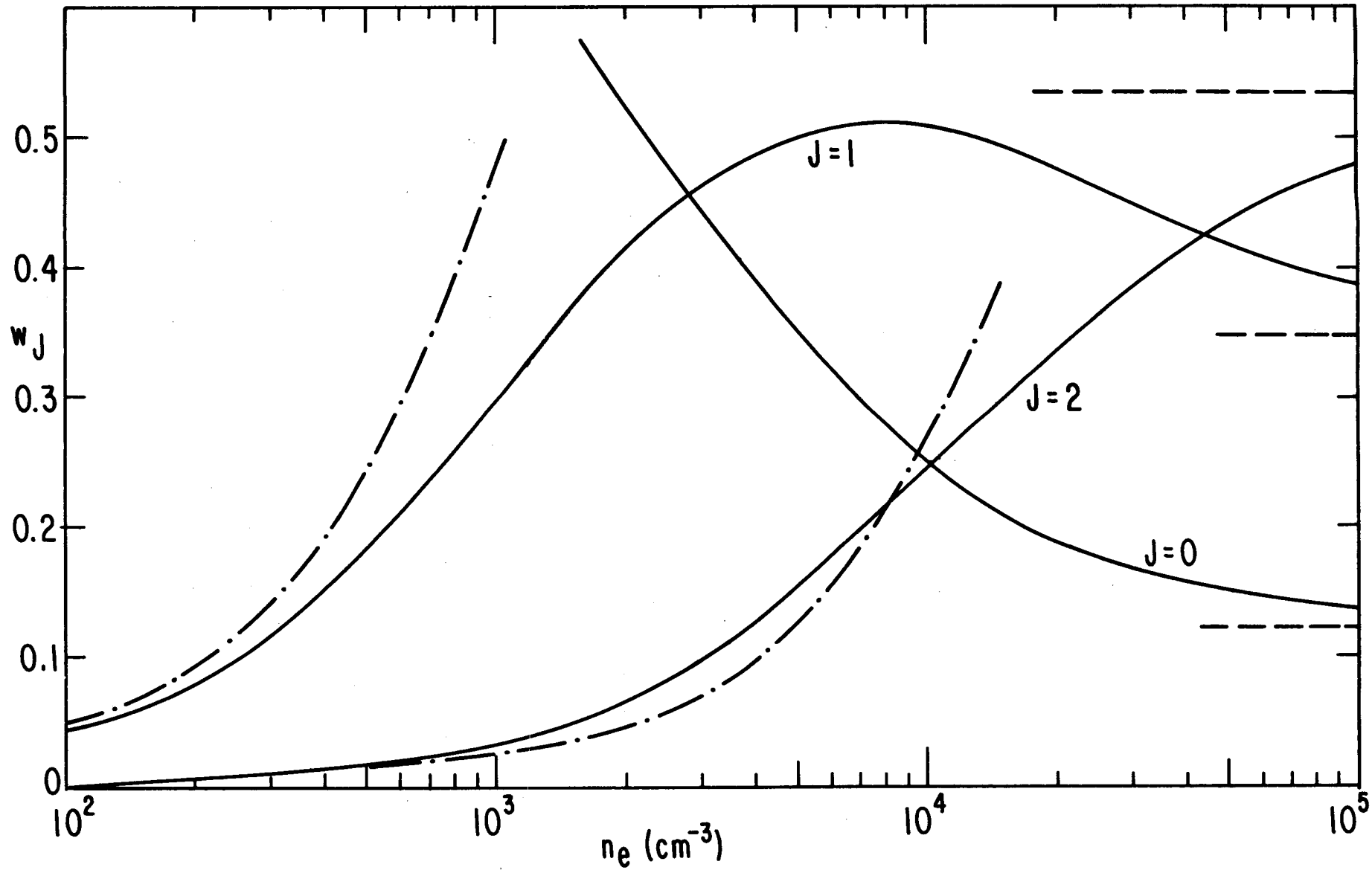

Fig. 1b

INFRARED LINE EMISSION FROM PLANETARY NEBULAE

II. CALCULATED SPECTRA OF NINE PLANETARIES

THOMAS N. DELMER and ROBERT J. GOULD

Department of Physics

University of California, San Diego

and

WILLIAM RAMSAY

Department of Physics

University of California, Santa Barbara

ABSTRACT

Estimates are given on the basis of optical data, of the expected infrared line intensities from nine bright planetary nebulae (see Table 4). There are a number of lines from these planetaries which should have intensities in the range 10^{-18} to 10^{-16} watts/cm^2. Ionized helium abundances and central star temperatures are derived for these planetaries. Also, improved estimates are given of the expected thermal bremsstrahlung radio emission from these nebulae, assuming that they are optically thin to radio radiation; comparison with radio observations indicates generally satisfactory agreement with these calculations.

I. INTRODUCTION

Applying the basic theory developed in the previous paper (Delmer, Gould, and Ramsay 1967, hereinafter referred to as "I"; we shall also refer to equations therein as, for example, (I-14)), we now proceed to estimate the intensities of lines in the infrared spectra of some of the brighter planetaries. We have chosen as subjects the planetary nebulae NGC 7027, IC 418, NGC 6572, NGC 6543, NGC 7662, NGC 7009, NGC 6826, NGC 6210, and NGC 6720. These planetaries, in the order given, have the largest absolute Hβ fluxes after correction for interstellar extinction, and were chosen from the list given by Osterbrock (1964). We have chosen from this list only the "small" planetaries subtending half-angles of less than about 10 seconds of arc; the more extended objects would not lie completely within the receptance cone of large telescopes. We have also concentrated on eleven lines (see Tables 3,4)from the nine species O IV, Ne II, Ne V, Mg IV, S III, S IV, A III, A V, and A VI. Once the parameters of the nebulae, the electron density and temperature, are determined, the infrared line intensities can be found from knowledge of the ionization conditions and from a measurement of the absolute intensity of some line, for example, Hβ. The central problem in the calculation of the infrared line spectra is that of estimating ionization conditions in the planetary. This is very difficult for most elements, since usually they exist in several stages of ionization, and in some stages there are no low lying optical levels and so no observable forbidden optical lines. However, in some cases an ion may have both low lying optical levels and ground state fine structure splitting; in this case the infrared line intensity from transitions between the fine structure levels may be estimated directly from the optical line

intensity from the same ion. In general, however, semi-theoretical calculations of ionization conditions are very difficult and thus must be regarded as only rough estimates. For this reason our predicted infrared line intensities in some cases must be regarded as only order of magnitude estimates. However, our purpose in this work is not to predict accurate values of the intensities but to give estimates to be used as a guide for future observational work. We emphasize that it is the observational results which will be of greatest value for the information they contain on element abundances. We hope that our theoretical work will serve as a useful guide in the interpretation of the observations.

In the following section (II) we shall indicate the sources of optical data on planetary nebulae and give our assumed parameters of the planetary such as the electron density and temperature. We shall also give the results of our determinations of the helium abundances and also our determinations of the temperatures of the central stars of the planetaries. In section III we discuss essentially our basis for estimating absolute line intensities from various planetaries; this is the data on absolute flux measurements of $H\beta$. We also give improved estimates of the radio thermal bremsstrahlung continuum fluxes expected in the optically thin regions of the radio spectra. The results of our calculations of the detailed infrared spectra are given in the last section (IV). As we shall show, there are a number of different lines from a number of planetaries which should have intensities in the range 10^{-18} to 10^{-16} Watt/cm^2. Present observations can detect signals of about 0.5×10^{-16} W/cm^2, while improved techniques could allow detection of signals as low as 10^{-18} W/cm^2.

II. OPTICAL DATA AND PARAMETERS OF PLANETARIES

We list in Table 1, for the planetaries under consideration, some important references for spectroscopic optical line intensity data; most of this work has been done by Aller and his collaborators. We make use of this data in making estimates of the ionization conditions in the planetaries. This data, along with determinations of the absolute $H\beta$ fluxes (see Table 2) allow estimates of the intensities of the infrared lines. In Table 1 we also list values of the electron density and temperature adopted in our calculations; these were taken from works by Aller (1956, 1964) and Seaton (1960). In some cases more accurate values of n_e and T_e could be derived from the more recent optical data. However, for our rough estimates of the expected infrared line intensities precise knowledge of these quantities is not required in most cases.

Also listed in Table 1 are the derived abundances of ionized helium relative to ionized hydrogen (actually, the ratio of the mean abundances weighted by the electron density, see I). These quantities were computed from equation (I-14) using the measured line intensities. The derived abundances quoted were determined, in the individual cases, from the spectroscopic data as given in the source listed first in Table 1; that is, for NGC 7027 the helium abundances were dervied from the data of ABW while for IC 418 the O'D data were used, etc. In making these choices of (hopefully) the best source of data we were guided by the measured values of $H\delta/H\beta$ and HeI λ 4026/λ 4471 which, according to theory, should be 0.26 and 0.46 respectively at $T_e = 10^4\ ^oK$. These line intensity ratios should be very weakly dependent on electron temperatures and for these relative helium abundance calculations we have taken $T_e = 10^4\ ^oK$ throughout. By comparison,

the average of the values for the adopted data sources is 0.24 and 0.50 respectively, in good agreement with theory, considering the uncertainties of measurements and approximations in the theory. The problem in determining the total (weighted) helium abundance is complicated by the fact that we have no way of measuring the amount of neutral helium. In low excitation planetaries like IC 418 the proportion of neutral helium should be appreciable while in high excitation planetaries like NGC 7027 and NGC 7662 the amount of neutral helium in the ionized regions should be small. One might argue that to evaluate the mean total helium abundance in planetaries one should take preferentially the higher total ionized helium values, since for these presumably the amount of neutral helium is small. The largest such value in Table 1 is 0.19 for NGC 6543. However, as we have emphasized, one really determines the ratio of the abundances integrated over the volume of the ionized region and weighted by the electron density. Thus, even if the helium abundance were exactly the same in each planetary, systematic density fluctuations would result in apparent differences in the total ionized helium abundance derived from the recombination spectra. In fact, for some planetaries such as NGC 7027 it is generally believed that there do exist considerable density fluctuations. On the basis of the data summarized in Table 1 we shall assume a total (neutral, singly and doubly ionized) helium to ionized hydrogen ratio of 0.18 for all planetaries. This hypothesis allows us to estimate the fraction of neutral helium in each planetary, which in turn allows estimates of ionization ratios in other elements.

For its great importance we have also evaluated the ionized helium abundance in the planetary nebula K648 in the globular cluster M15. The importance of this planetary lies in the fact that, being a "halo" object, its element abundance may be representative of primordial matter. Using the line

intensity measurements of O'Dell, Peimbert, and Kinman (1964), we find $\langle n_e n_{He^+} \rangle / \langle n_e n_{H^+} \rangle = 0.147$, and $\langle n_e n_{He^{+2}} \rangle / \langle n_e n_{H^+} \rangle < 0.025$. It appears that the helium abundance in this planetary is "normal" in striking contrast to the oxygen to hydrogen abundance ratio which is down from the solar value by a factor of 60. It is clear that this result has bearing on the recent determinations of the helium abundance in the atmospheres of halo horizontal branch stars by Sargent and Searle (1966).

Finally, in Table 1 we give the results of our determinations of the temperatures of the central stars of the planetaries. These results are derived from the ionized helium to hydrogen ratios, that is, essentially from the measured intensities of Hβ, HeI λ4471, and HeII λ4686 (see eq. (I-14)). The temperatures are derived from the basic relations (I-16) and (I-17). When good measures of the He^{+2} abundances from the HeII λ4686 line were available, this density relative to hydrogen was used to determine the temperature T_o, since this ratio has a strong dependence on T_o. In other cases the temperatures were determined from measures of the He^{+} abundances. We should emphasize that the temperatures derived in this manner are <u>not</u> dependent on the magnitude of the density fluctuations in the planetary. This is so essentially because both the total recombination rate and total rate of production of the associated recombination lines involves the same type integral over the volume of the ionized region of the planetary. We compare our results for T_o with those of Harmon and Seaton and of O'Dell; comparison of our basic <u>methods</u> is given in I. Disagreement with the Harmon-Seaton results is never very large, but we disagree by a factor of two with the value derived by O'Dell for NGC 7662. We feel our value is more reasonable, in view of the fact that this nebula is known to be a high excitation object. Moreover, we feel that O'Dell's determinations may be in error due to a numerical mistake in the basic equation (4)

of his paper. We were unable to reproduce the derived value of the constant term in this equation. The equation is definitely inconsistent with his equation (2) with the value of the constant therein.

III. IONIZATION MEASURE

In the low density limit where collisional de-excitation is negligible, the observed intensity of both collisionally excited lines and lines resulting from radiative capture and cascade is given by an expression of the form

$$J_\ell = \frac{e^{-\tau_\ell}}{4\pi d^2} \int n_e n_i \varepsilon_\ell dV \; ; \tag{1}$$

here τ_ℓ is the interstellar and atmospheric absorption optical depth, d is the distance to the planetary, $n_e n_i \varepsilon_\ell$ is the energy production rate per cm^3 for the line (cf. eq. (I-11)), and the integral is over the ionized volume of the nebula. In the case of collisional excitation n_i is the density of the ion from which the line is emitted; when the line results from radiative recombination, n_i is the density of the recombining ion. It is clear that, given the abundance of the ion relative to hydrogen, the line intensity is determined essentially by the amount of ionization

$$I = \int n_e n_{H^+} \, dV \; , \tag{2}$$

if the atomic rate constant ε_ℓ is known. The quantity I/d^2 can be computed from observational data in two ways: (1) from measurement of the absolute $H\beta$ flux and (2) from measurement of the radio thermal bremsstrahlung from the nebula. Each method has a drawback; method (1) requires correction for interstellar extinction, while method (2) requires a correction if the nebula is not optically thin to radio radiation; method (2) also requires a correction

for the contribution of ionized helium to the thermal bremsstrahlung. We have chosen to employ method (1) using absolute Hβ fluxes, corrected for interstellar extinction (Osterbrock 1964). However, we shall also make some comparison with the radio measurements.

As we have shown in I (eq. (I-11)), for Hβ emission the temperature dependence of the parameter ε_β is

$$\varepsilon_\beta = A_\beta \, T_e^{-1/2} \, \ell n \, \beta_e \tag{3}$$

where A_β is a constant (0.449×10^{-23} c.g.s. units) and $\beta_e = I_H/kT_e$. This simple form (3) is very useful, and represents the temperature dependence of Hβ emission very well in the temperature range corresponding to planetary nebulae. We have employed this equation, using the electron temperatures given in Table 1 and the observed corrected Hβ fluxes, to determine essentially the quantity I/d^2. The problem of estimating the ion abundance n_i/n_{H^+} involves procedures differing in detail for the different planetary nebulae. We shall discuss some individual cases in the following section.

For the case of an optically thin nebula there is a very simple relationship between the intensity of the radio thermal bremsstrahlung spectral continuum $F_{B,\nu}$ (in ergs/cm^2-sec-Hz) and the total intensity $I_{H\beta}$ (in ergs/cm^2-sec), of the Hβ line, corrected for interstellar extinction. Using the Born approximation bremsstrahlung cross section to calculate the spectral radio emission from $e\text{-}H^+$, e, He^+, and $e\text{-}He^{+2}$ encounters (cf. Tucker and Gould 1966) one finds, in c.g.s. units,

$$\frac{F_{B,\nu}}{I_{H\beta}} = 0.805 \times 10^{-14} \left(1 + \frac{\langle n_e n_{He^+} \rangle}{\langle n_e n_{H^+} \rangle} + 4 \frac{\langle n_e n_{He^{+2}} \rangle}{\langle n_e n_{H^+} \rangle} \right) \frac{\ell n \, \alpha_\nu}{\ell n \, \beta_e} \tag{4}$$

where $\alpha_\nu = 2kT_e/\pi\Gamma h\nu$ with $\ln\Gamma = 0.5772$ (Euler's constant); it has been assumed that there are no large temperature variations in the nebula. The magnitude of the terms in parentheses in equation (4) may be found for the individual planetary from measurements of helium to hydrogen line intensity ratios, using equations (I-14). Thus, from a knowledge of the absolute $H\beta$ flux $I_{H\beta}$ from the planetary and from measurements of HeI and HeII recombination line intensities relative to $H\beta$ one can compute the expected intensity of the radio continuum; this has been done by Osterbrock (1964). We have repeated his calculations, making use of our equation (4); it should be noted that, since α_ν , $\beta_e \gg 1$, the dependence on electron temperature of our calculated ratio (4) is very weak. Our calculations should be somewhat more accurate than Osterbrock's, due essentially to use of our accurate expression (3) for $H\beta$ emission and our more accurate inclusion of the effect of ionized helium. We give in Table 2 the results of these calculations, using the absolute $H\beta$ fluxes given by Osterbrock (loc. cit.) and the data in Table 1. Our $F_{B,\nu}$ is calculated for $\nu = 3000$ MHz which is the highest frequency at which there is extensive radio observations of planetaries; it is compared with the observations (Menon and Terzian 1965) at this frequency and with the calculations of Osterbrock at 1400 MHz. The difference in the calculated values due to the different frequencies adopted amounts to only about 5% (exact dependence as in eq. (4), $F_{B,\nu}$ slightly lower at higher frequencies). We see that our calculated value is always larger than Osterbrock's and always larger than the observational value. That the observational values are lower should certainly be the case, since we have assumed that the nebula is optically thin, and some of the radiation, even at such high frequencies, is being absorbed in the nebula. In fact, from the frequency plots of data at 750, 1410, and 3000 MHz by Menon and Terzian it is

clear that some of the nebulae are not optically thin at 3000 MHz. Specifically, NGC 7027, IC 418, and NGC 6572 definitely do not appear to have spectra characteristic of optically thin objects, so it is not surprising that the observational $F_{B,\nu}$ is smaller than the calculated value. Moreover, the observation of NGC 6543 at 3000 MHz seems suspect when compared with the observations at lower frequencies. Thus, one can account for all the large discrepancies in Table 2 between calculations and observations. On the other hand, for NGC 6720 radio observations indicate that the nebula is optically thin and we also see from Table 2 that our calculated radio intensity at 3000 MHz agrees well with the observed value. In summary, it appears that the general radio observations of thermal bremsstrahlung from planetaries can be understood on the basis of the observed optical recombination spectra. Undoubtedly, further information on the structure of planetaries not optically thin to radio radiation may be gained from more detailed analysis of this data; this is not the subject of this paper, however.

IV. CALCULATED SPECTRA

a) Atmospheric Transmission

The transmission of the atmospheric gases in the infrared region is a difficult problem to treat theoretically because the photon absorption takes place within the quite complex vibration - rotation bands of (principally) water vapor and CO_2 and (less importantly) NO_2, O_3, and CH_4. Only experimental results are reliable at present for quantitative work; furthermore, the experimental absorption values themselves may be easily contaminated by the presence of dust or by a non-uniform distribution of water vapor; in addition, the typically extreme jaggedness of measured absorption curves suggests that measurements at a given wavelength may be quite dependent on

bandwidth. Therefore, it is not surprising that experimental results are sometimes conflicting; examples of these conflicts are discussed below. It seems, really, that there is no substitute at present for an independent calibration of infrared transmission for each experiment; such a calibration, involving fitting the observed moon i-r spectrum to a black-body model, is described in Sinton and Strong (1960). It may be helpful, however, to give our best estimates, derived from various experiments, of the atmospheric transmission T for the infrared lines we consider. Table 3 gives the values of T calculated from the relation

$$\ell_n T = - \alpha w - \beta w^{1/2}, \qquad (5)$$

where α and β are constants, and w is the amount of precipitable water in the atmospheric path: w = water (pr.mm) $\approx$ 10 at the zenith. The values of α and β are taken from the various sources as given below.

4.492μ and 4.525μ: Gates and Harrop, 1963. The α value is that which they define as "continuous" absorption, the β is their fit of the "selective" absorption data to the "strong random band model". (See their paper for a discussion).

7.893μ: Gates and Harrop again, but this time their best fit is to $\beta = 0$ and α equal to a continuous plus selective absorption. This is the weak random band model, in this approximation, of course, Lambert's Law of exponential absorption.

8.990, 10.53, and 12.8μ: Anthony (1952). Here absorption is small and the exponential law should hold. The two smaller wavelengths are dominated by the "continuous" absorption in Gates and Harrop and do not agree with these; agreement with Bignell et al. (1963) is good. The absorption in the region of the 12.8μ line, not treated by Gates and Harrop, is larger in Bignell et al. Anthony's experimental point, however, is right at our line, a distinction which may be important.

13.1μ: Farmer and Key (1965) give values for this region of the spectrum. However, they admit that all their transmissions at these wavelengths may be low, so that we have adopted their 13.1μ to 12.8μ ratio and then scaled an $\alpha_{13.1}$ using Anthony's $\alpha_{12.8}$. (Their absorption curves shapes are smaller for these two, CO_2 absorption not yet being very large at 13.1μ.)

18.68μ: interpolated from Anthony (1952). This is again a smaller absorption than Bignell et al. or Farmer and Key.

21.84μ, 24.2μ, 25.87μ: Farmer and Key have a near monopoly on data here, and their single points are (very tentatively) fitted to a strong-random band model (suitable to high absorption regions). There is the additional difficulty here that their spectra tracings show our two longest lines very near big absorption peaks, so that small Doppler shifts or a widening of bands with increase of water vapor may greatly change the transmission value.

b) Infrared Line Spectra

Table 4 lists the calculated values of the line intensities for the nine planetaries considered here. Line intensities are listed only when their estimated values exceed 10^{-18} W/cm^2. The first column gives the atmospheric transmission for w = 10 pr.mm at the wavelength of the line, i.e. the factor by which the tabulated intensities must be multiplied to give the expected intensities at a ground based observation point. Parentheses indicate intensity values which may be off by a large factor (sometimes exceeding 30). Such large errors would be due to uncertainties in the determination of the abundance of the radiating ion (see Introduction).

In cases where the infrared line intensities can be estimated from optical observations of forbidden lines of the same ion, the values should

be accurate, since such observations give a measure of the abundance of the ion in a region of low enough electron density to allow forbidden line emission. In contrast, recombination lines may not be a measure of the abundance of ions capable of forbidden line emission. Indeed Aller (1964) comments that for NGC 6572 part of the O line intensities used in his calculations of the O abundance may not originate entirely in the nebula, but may come from the central star. The few ions which emit both infrared and optical forbidden radiation are S^{+2}, Ne^{+4}, A^{+2}, A^{+4} and observational data are not always available for these. Thus, in many cases, another, less accurate method must be used. The other method (giving rise to the values of Table 4 listed in parentheses) is one of comparison of the relative abundance of ions of one element with the known relative ionic abundance of another element (here either O or He) using equations (I-1) and (I-6). The ionic abundances of He are listed in Table 1; O^{+} and O^{+2} abundances can be gotten from their forbidden line radiation; in some cases, Aller (1964) has computed the ionic abundances of O. Once comparison gives the relative ionic abundances of an element, the ionic abundance can be fixed either by fixing the abundance of one ion from its forbidden line emission, or, in the case where there are no observations of forbidden lines, by assuming a total abundance for the element. In the latter case Aller's (1964) abundances were used. The ionic abundance is then used to determine the intensity.

For the calculation of relative abundances of ions like S^{+2}, A^{+2}, and A^{+4} from optical forbidden line data it is necessary to know the relevant atomic collision strengths. As yet, calculations for $3p^q$ configuration have only been done for S^{+} by Seaton (1958). We have estimated the collision strengths for other ions $X^{+Q} : 3p^q$ by comparison with the Ω's for the corresponding ion $Y^{+Q} : 2p^q$ in the $2p^q$ configuration. That is, we take

$$\frac{\Omega(X^{+Q} : 3p^q)}{\Omega(S^{+} : 3p^3)} \approx \frac{\Omega(Y^{+Q} : 2p^q)}{\Omega(O^{+} : 2p^3)} \quad , \tag{6}$$

using the results of Seaton's (loc. cit.) calculations for S^+, O^+, and Y^{+Q}.

In the second method comparisons can be made in several ways. For example, consider the problem of determining the ionic abundance of Ne^+ in IC 418. Low (unpublished) has observed a flux of about 10^{-16} W/cm^2 from this planetary near 13μ. This has been interpreted earlier (Gould 1966) as Ne II emission. From comparison with O^+/O^{++} derived from forbidden lines, one gets $Ne^+/Ne^{++} \approx 5$. Similarly, from a comparison with He^0/He^+ one gets $Ne^0/Ne^+ \approx .3$ indicating Ne is mostly singly ionized. Using Aller's total Ne abundance and this latter ratio, one then gets the intensity listed in Table 1 which agrees with the observations. However, if one uses the observed NeIII abundance as derived from an observed forbidden line, one gets an intensity which is 100 times less (this would also indicate Ne to be underabundant by a factor of 100). This result probably arises from a combination of inaccuracies in the atomic constants used in the calculation (mainly photoionization cross sections) and deviation from the simple homogeneous model assumed for all the planetaries.

Realizing the possibility of such large errors, the line intensities were calculated keeping in mind that neither large deviations from the average abundances are to be expected, nor are deviations from the excitation of the planetary as indicated by the temperature of the central stars to be expected. Thus one would expect less Ne^{++} than Ne^+ in the low excitation planetary IC 418. Similarly one would expect less S^{+++} than S^{++} in NGC 6210 even though comparison with O^{++}/O^+ would suggest the contrary. There was in this case no other reasonable means of computing the ionic abundance of S. Such inconsistencies lead one to expect a large error in some cases. However, whenever more than one method of calculation was available, the most 'reasonable' value was selected.

Finally, a plot of the infrared spectrum of NGC 7027 in the region of

the forbidden line emission is shown in Figure 1. The plot demonstrates how the lines stand out above the Bremsstrahlung continuum. Note that for this planetary the background continuum should be observable, as indicated by Stein (1967). For the purposes of plotting, the line shapes were assumed to be flat over a Doppler width corresponding to $\pm$ 35 km/sec. The study of line profiles in planetaries by Osterbrock, Miller and Weedman (1966) indicates that this is a reasonable broadening to expect.

We have benefited from conversations with F. J. Low, W. G. Mathews, and W. A. Stein. This work was supported in part by the National Science Foundation and in part by NASA through Grant NsG-357.

Table 1. DATA ON PLANETARY NEBULAE

Planetary Nebula	Sources of Spectral Data	Electron Density n_e ($10^4 cm^{-3}$)	Electron Temperature T_e (10^4 °K)	Derived Helium Abundances		Derived Central Star Temperature T_o		
				$\frac{\langle n_e n_{He^+} \rangle}{\langle n_e n_{H^+} \rangle}$	$\frac{\langle n_e n_{He^{+2}} \rangle}{\langle n_e n_{H^+} \rangle}$	This Work (10^4 °K)	Harmon and Seaton (1966) (10^4 °K)	O'Dell (1963b) (10^4 °K)
NGC 7027	ABW, LA, O'D, ABM	2	1.55	0.120	0.033	11.8		
IC 418	O'D, AK_c, LA	1.6	1.83	0.123	. . .	3.87	4.26	5.3
NGC 6572	AK_b, LA	1.0	1.13	0.120	. . .	4.24	6.16	6.4
NGC 6543	O'D, LA	1.5	0.95	0.190	0.001	6.31	6.60	5.3
NGC 7662	AKB, LA, O'D, MA	0.9	1.3	0.076	0.051	13.8	10.0	6.2
NGC 7009	AK_a, LA	0.6	1.13	0.144	0.015	9.51	8.1	5.6
NGC 6826	O'D, LA	0.22	1.12	0.162	. . .	4.22	6.9	4.2
NGC 6210	LA	0.9	1.08	0.167	. . .	4.25	5.0	5.8
NGC 6720	AW, LA	0.10	1.3	0.117	0.011	8.98		13.2

ABW : Aller, Bowen, and Wilson (1963)

LA : Liller and Aller (1963)

O'D : O'Dell (1963a)

ABM : Aller, Bowen, and Minkowski (1955)

$AK_{a,b,c}$: Aller and Kaler (1964a, b, c)

AKB : Aller, Kaler, and Bowen (1966)

AW : Aller and Walker (1965)

MA : Minkowski and Aller (1956)

Table 2. RADIO CONTINUUM EMISSION FROM PLANETARIES

Nebula	$\log I_{H\beta}$ (ergs/cm^2-sec) (Osterbrock 1964)	$F_{B,\nu}$ (10^{-26} W/m^2 - Hz)		
		Obs., ν=3000 MHz (Menon and Terzian 1965)	Calc., ν=3000 MHz (this work)	Calc., ν=1400 MHz (Osterbrock 1964)
NGC 7027	- 8.78	6.2	9.1	6.2
IC 418	- 9.06	1.6	4.8	3.2
NGC 6572	- 9.22	1.0	2.5	2.2
NGC 6543	- 9.32	0.9	2.0	1.8
NGC 7662	- 9.56	0.9*	1.4	1.0
NGC 7009	- 9.66	0.8	0.99	0.8
NGC 6826	- 9.68		0.86	0.8
NGC 6210	- 9.76		0.74	0.6
NGC 6720	- 9.91	0.55*	0.57	0.4

* extrapolated from lower frequencies.

Table 3. ATMOSPHERIC ABSORPTION PARAMETERS

Transition (ion: $J_1 \rightarrow J_2$)	λ (microns)	α $(\text{pr mm})^{-1}$	β $(\text{pr mm})^{-1/2}$	T for w=10 pr mm.
M_gIV: $\frac{1}{2} \rightarrow \frac{3}{2}$	4.492	0.012	0.79	0.07
A VI: $\frac{3}{2} \rightarrow \frac{1}{2}$	4.525	0.012	0.71	0.09
A V: $2 \rightarrow 1$	7.893	0.12	0	0.30
A III: $1 \rightarrow 2$	8.990	0.0067	0	0.94
S IV: $\frac{3}{2} \rightarrow \frac{1}{2}$	10.53	0.0064	0	0.94
N_eII: $\frac{1}{2} \rightarrow \frac{3}{2}$	12.8	0.012	0	0.89
A V: $1 \rightarrow 0$	13.1	0.11	0	0.33
S III: $2 \rightarrow 1$	18.68	0.096	0	0.38
A III: $0 \rightarrow 1$	21.8	0	1.2	0.02
N_eV: $1 \rightarrow 0$	24.2	0	0.85	0.07
O IV: $\frac{3}{2} \rightarrow \frac{1}{2}$	25.87	0	1.2	0.02

Table 4. EXPECTED INFRARED LINE INTENSITIES FROM PLANETARY NEBULAE

Transition (ion: $J_1 - J_2$)	Wave number $\tilde{\nu}$ (cm^{-1})	Wave length λ (microns)	Atmospheric transmission T	Energy flux before transmission through atmosphere (10^{-16} watts/cm^2)								
				NGC 7027	IC 418	NGC 6572	NGC 6543	NGC 7662	NGC 7009	NGC 6826	NGC 6210	NGC 6720
O IV: $\frac{3}{2} - \frac{1}{2}$	386.5	25.873	0.02	(40)	-	(0.01)	(0.01)	(0.5)	(0.2)	-	-	(2)
Ne II: $\frac{1}{2} - \frac{3}{2}$	782	12.79	0.89	(0.04)	(3)	(0.3)	(0.05)	-	(0.01)	(0.5)	(0.4)	(0.06)
Ne V: 1 - 0	414	24.15	0.07	0.5	-	-	-	0.04	-	-	-	-
Mg IV: $\frac{1}{2} - \frac{3}{2}$	2226	4.492	0.07	(0.02)	-	-	-	(0.02)	(0.02)	-	-	-
S III: 2 - 1	535.3	18.681	0.38	0.5	0.1	0.1	0.1	0.03	0.1	-	(0.2)	(0.02)
S IV: $\frac{3}{2} - \frac{1}{2}$	950.2	10.524	0.94	(1)	-	(0.2)	(1)	(1)	(0.8)	(0.07)	(1)	(0.01)
A III: 0 - 1	457.80	21.8436	0.02	0.2	0.02	0.2	0.07	0.01	0.04	-	(0.02)	(0.02)
A III: 1 - 2	1112.40	8.98957	0.94	0.7	0.1	0.7	0.3	0.04	0.1	0.01	(0.08)	(0.05)
A V: 1 - 0	765	13.07	0.33	0.2	-	-	-	(0.06)	(0.1)	-	-	-
A V: 2 - 1	1267	7.893	0.30	0.2	-	-	-	(0.05)	(0.07)	-	-	-
A VI: $\frac{3}{2} - \frac{1}{2}$	2210	4.525	0.09	(0.06)	-	-	-	-	-	-	-	-

REFERENCES

Aller, L. H. 1956, Gaseous Nebulae (New York: John Wiley).

_____ 1964, P.A.S.P., 76, 279.

Aller, L. H., Bowen, I. S., and Minkowski, R. 1955, Ap. J., 122, 62.

Aller, L. H., Bowen, I. S., and Wilson, O. C. 1963, Ap. J., 138, 1013.

Aller, L. H. and Kaler, J. B. 1964a, Ap. J., 139, 1074.

_____ 1964b, ibid., 140, 621.

_____ 1964c, ibid., 140, 936.

Aller, L. H. and Walker, M. F. 1965, Ap. J., 141, 1318.

Anthony, R. 1952, Phys. Rev., 85, 674.

Bignell, K., Saiedy, F., and Sheppard, P. A. 1963, J. Opt. Soc. Amer., 53, 466.

Delmer, T. N., Gould, R. J. and Ramsay, W. 1967, Ap. J., (previous paper).

Farmer, C. B. and Key, P. J. 1965, Applied Optics, 4, 1051.

Gates, D. M. and Harrop, W. J. 1963, Applied Optics, 2, 887.

Gould, R. J. 1966, Ap. J., 143, 603.

Harmon, R. J. and Seaton, M. J. 1966, M. N., 132, 15.

Liller, W. and Aller, L. H. 1963, Proc. Nat. Acad. Sci., 49, 675.

Menon, T. K. and Terzian, Y. 1965, Ap. J., 141, 745.

Minkowski, R. and Aller, L. H. 1956, Ap. J., 124, 93.

O'Dell, C. R. 1963a, Ap. J., 138, 1018.

_____ ibid., p. 67.

O'Dell, C. R., Peimbert, M., and Kinman, T. D. 1964, Ap. J., 140, 119.

Osterbrock, D. E. 1964, Ann. Rev. Astron. and Astrophys., 2, 95.

Osterbrock, D. E., Miller, S. J., and Weedman, D. W. 1966, Ap. J., 145, 697.

Sargent, W. L. W. and Searle, L. 1966, Ap. J., 145, 652.

_____ 1960, Rept. Prog. Phys., 23, 313.

Seaton, M. J. 1958, Rev. Mod. Phys., 30, 979.

Sinton, W. M. and Strong, J. 1960, Ap. J., 131, 459.

Stein, W. A. 1967, Ap. J. (in press).

Tucker, W. H. and Gould, R. J. 1966, Ap. J., 144, 244.

FIGURE CAPTIONS

Fig. 1. Computed line spectrum of NGC 7027 plotted along with the thermal bremsstrahlung continuum. Line widths were computed assuming a simple rectangular line shape over wavelengths corresponding to Doppler shifts over $\Delta v = \pm 35$ km/sec.

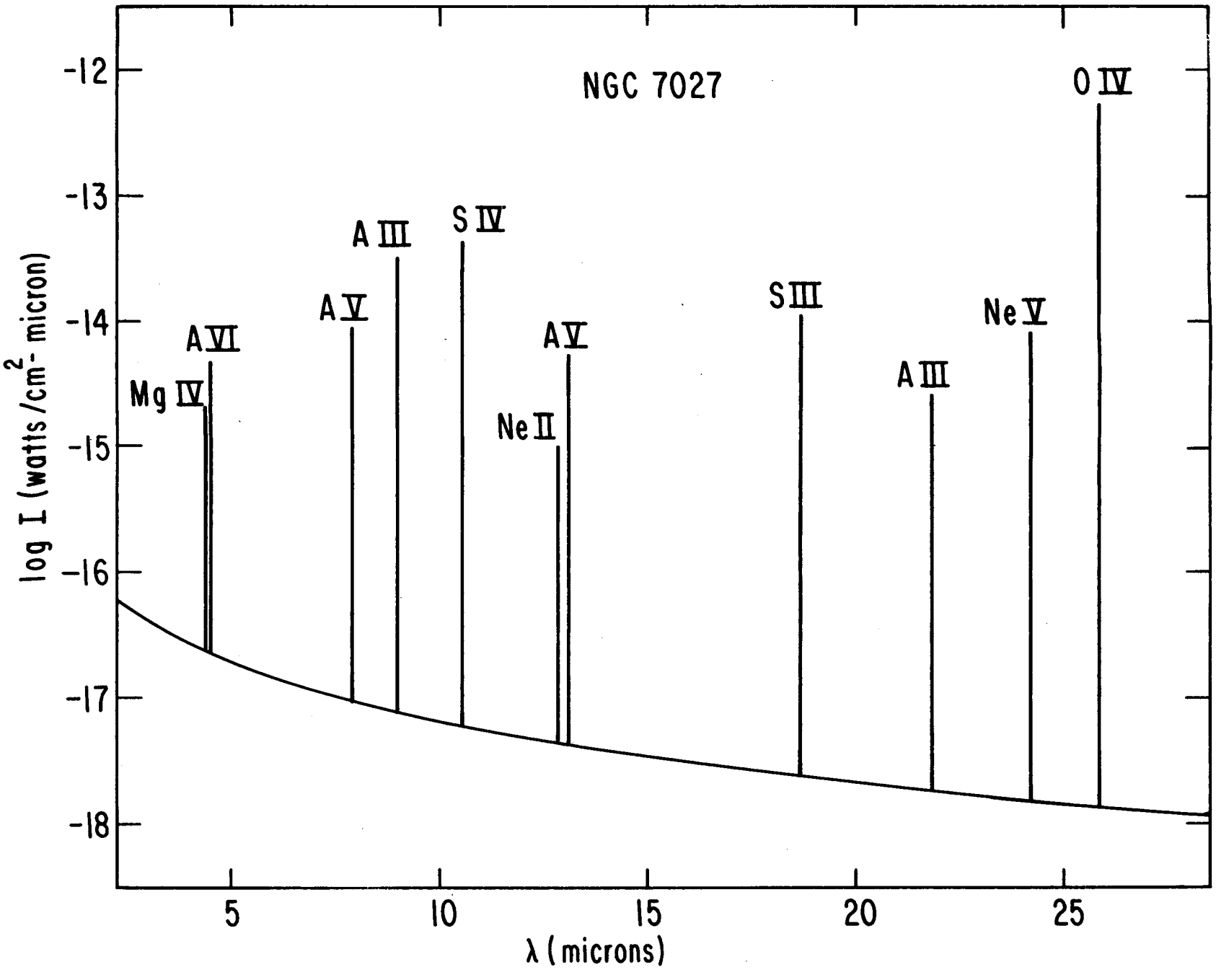
NGC 7027
log I (watts/cm^2- micron)
λ (microns)
-12
-13
-14
-15
-16
-17
-18
5
10
15
20
25
Mg IV
A VI
A V
A III
S IV
Ne II
A V
S III
A III
Ne V
O IV

Fig. 1